

REPORT DOCUMENTATION PAGE					<i>Form Approved</i> OMB No. 0704-0188	
The public reporting burden for this collection of information is estimated to average 1 hour per response, including the time for reviewing instructions, searching existing data sources, gathering and maintaining the data needed, and completing and reviewing the collection of information. Send comments regarding this burden estimate or any other aspect of this collection of information, including suggestions for reducing the burden, to Department of Defense, Washington Headquarters Services, Directorate for Information Operations and Reports (0704-0188), 1215 Jefferson Davis Highway, Suite 1204, Arlington, VA 22202-4302. Respondents should be aware that notwithstanding any other provision of law, no person shall be subject to any penalty for failing to comply with a collection of information if it does not display a currently valid OMB control number. PLEASE DO NOT RETURN YOUR FORM TO THE ABOVE ADDRESS.						
1. REPORT DATE (DD-MM-YYYY) 05-11-2014		2. REPORT TYPE Final			3. DATES COVERED (From - To) 5 March 2013 - 4 April 2014	
4. TITLE AND SUBTITLE Multi-functional Infrared Sensor				5a. CONTRACT NUMBER FA2386-13-1-4025		
				5b. GRANT NUMBER Grant 13RSZ057_134025		
				5c. PROGRAM ELEMENT NUMBER 61102F		
6. AUTHOR(S) Professor Sang Jun Lee				5d. PROJECT NUMBER		
				5e. TASK NUMBER		
				5f. WORK UNIT NUMBER		
7. PERFORMING ORGANIZATION NAME(S) AND ADDRESS(ES) Korea Research Institute of Standards and Science 267 Gajeong-Ro, Yuseong-Gu Daejeon 305-340 Korea					8. PERFORMING ORGANIZATION REPORT NUMBER N/A	
9. SPONSORING/MONITORING AGENCY NAME(S) AND ADDRESS(ES) AOARD UNIT 45002 APO AP 96338-5002					10. SPONSOR/MONITOR'S ACRONYM(S) AFRL/AFOSR/IOA(AOARD)	
					11. SPONSOR/MONITOR'S REPORT NUMBER(S) 13RSZ057_134025	
12. DISTRIBUTION/AVAILABILITY STATEMENT Distribution Code A: Approved for public release, distribution is unlimited.						
13. SUPPLEMENTARY NOTES						
14. ABSTRACT The purpose of the project is to develop plasmonic couplers and infrared detectors to realize multi-functional infrared sensors. The PI investigated in analyzing a novel detector structure for pixel-level multi-spectral infrared imaging; perforated gold films with Si ₃ N ₄ overlayers, studied the fundamental understanding of surface plasmon polariton modes and their angle dependence; the effect of confinement barriers of InAs/InGaAs sub-monolayer (SML) quantum dots-in-a-well based infrared photodetectors; and characterization of multi-stack InAs/InGaAs SML quantum dots (QDs) that are grown via Stranski-Krastanov growth method. The project demonstrated the first monolithically integrated plasmonic infrared quantum dot pixelated focal plane array (FPA) to enhance the performance at specific wavelengths. The project continued to be supported to develop four different plasmonic patterns the FPA.						
15. SUBJECT TERMS plasmonics, quantum dot detector, Microwave Infrared						
16. SECURITY CLASSIFICATION OF:			17. LIMITATION OF ABSTRACT	18. NUMBER OF PAGES	19a. NAME OF RESPONSIBLE PERSON	
a. REPORT	b. ABSTRACT	c. THIS PAGE			Misoon Y. Mah, Ph.D.	
U	U	U	SAR	10	19b. TELEPHONE NUMBER (Include area code) +81-42-511-2000	

Final Report

PROJECT TITLE: Multi-functional Infrared Sensor (AOARD 134025)

PRINCIPAL INVESTIGATOR:

Dr. Sang Jun Lee, Principal Research Scientist

Email: silee@kriss.re.kr, Phone: +82 42 868 5127, Fax: +82 42 868 5047

Address: Korea Research Institute Standards and Science, 267 Gajeong-Ro, Yuseong-Gu, Daejeon 305-340, Rep. of Korea

I. INTRODUCTION

The Korean Research Institute of Standards and Science (KRISS) teamed up with the Air Force Research Laboratory (AFRL) on a project titled “Multi-functional Infrared Sensor”. The first year of the project was a resounding success. There were not only significant advances in both science and technology (as outlined in the following sections), but there was a very healthy interaction between fabrication & measurement parts carried out at KRISS and design & simulation parts performed at AFRL to achieve the multi-functional infrared sensors by plasmonics.

The intimate collaboration between the AFRL and KRISS has resulted in publications and presentations, for example *Optical Materials Express* **4**, 198-204 (2014), *Journal of Applied Physics* **115**, 163101 (2014), the International Materials Research Congress in Cancun, Mexico (Aug 2013), International Symposium on the Physics of Semiconductors and Applications in Jeju, Korea (Dec 2013), etc.

II. ACCOMPLISHMENTS

We have made significant progress in both plasmonic couplers and infrared detectors toward the realization of multi-functional infrared sensor.

- a. A novel detector structure for pixel-level multi-spectral infrared imaging was proposed and analyzed. More specifically, we investigated the device performance of a grating-integrated quantum dots-in-a-well photodetector under backside illumination. It can be expected that our design uses 1-dimensional grating patterns fabricated directly on a semiconductor contact layer, and thus adds a minimal amount of additional effort to conventional detector fabrication (Published in *Journal of Applied Physics*).
- b. A perforated gold film (used as surface plasmon resonance structure) with Si_3N_4 overlayers (used as antireflection coating layer) was investigated for the selective and the enhanced transmission in the mid- and long-wave infrared regions. Also, maximum transmission condition was analyzed numerically by using three layer model at which transfer matrix method is used to calculate the total reflection (In preparation for *Applied Physics Letters*).
- c. In order to realize the multi-functional infrared FPA or to improve the FPA device

performance using plasmonic couplers for IR management architecture, it is important to investigate the angle dependence of plasmonic structures due to thermal imaging camera lens, which is essential tool for IR images. Therefore, we studied the underlying mechanism of surface plasmon polariton modes and their angle dependence by means of experiment, theory and simulation (In preparation for IEEE Electronics Letters).

d. We reported the effect of confinement barriers on the performance of InAs/InGaAs sub-monolayer (SML) quantum dots-in-a-well based infrared photodetectors, which resulted in reduced dark current and improved detectivity performance, and wavelength tunability (Published in *Optical Materials Express*).

e. The structural characterization of multi-stack InAs/InGaAs SML quantum dots (QDs) grown under Stranski-Krastanov growth mode was performed through in-plane and out-plane polarization dependent study. The lateral quantum confinement in 3-6 stacks SML QDs was inferred from the polarization dependent response and the STEM image exhibiting the interdiffusion of indium atoms between SML-QDs and InGaAs quantum well as a result of insufficient amount of indium (In preparation for *Applied Physics Letters*)

f. The substrate removal using mechanical, chemical and dry etch processes has been optimized.

III. DETAILED RESULTS

1. Simulation and analysis of grating-integrated quantum dot infrared detectors (Section II-a)

Figure 1(a) shows a schematic of the IR photodetector structure that we studied (note that only one unit cell is shown here). Such structures can be made by substrate removal and patterning of a grating structure on the surface of the flipped semiconductor contact layer. We show that we can gain wide-range control of spectral response as well as large overall detection enhancement by adjusting grating parameters. We represent the overall device performance (ODP) data using a 2D color map as shown in Figure 1(b). It clearly shows how the ODP changes with grating parameters for broad, unpolarized IR radiation (i.e. under a realistic measurement condition). The p and d/p values producing the same ODP are indicated as dotted contour lines. As the grating period p increases, we have more response peaks, and the ODP increases (i.e. the color changes from blue to red). The ODP can reach beyond 3, depending on grating parameters. Although we only obtain a tiny ODP enhancement for small periods (around $p \sim 1 \mu\text{m}$), it is still valuable for spectral response control (not shown here). Our work clearly demonstrates that simple 1D structures provide significant control of spectral response and detection enhancement. We expect our design and analysis can lead to IR photodetectors useful for various IR imaging applications.

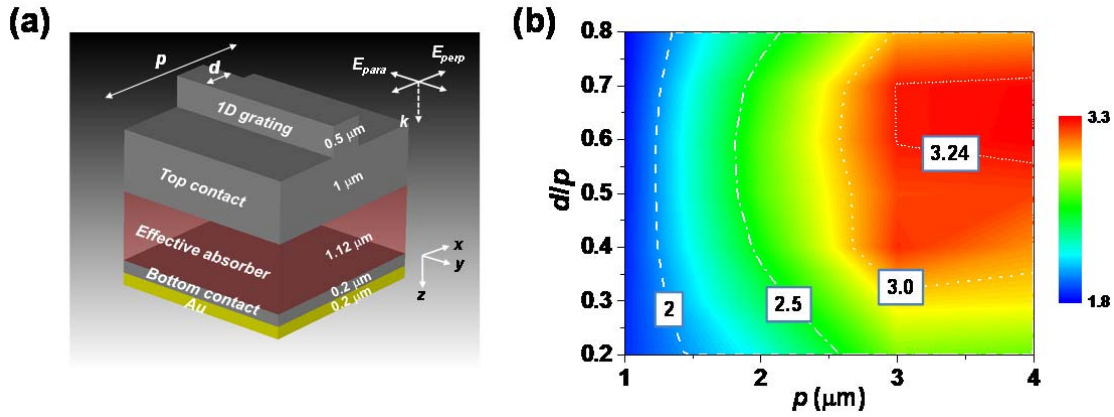


Figure 1 | (a) Schematic of a grating-integrated DWELL IR detector. (b) A 2-dimensional color map of the overall device performance (ODP) for unpolarized light as a function of the grating period p and the ratio d/p .

2. Enhanced transmission through 2D-MHA with Si_3N_4 antireflection coating layer (Section II-b)

SP resonance structures for the selective and the enhanced transmission of infrared light were designed. In order to relieve the large discontinuity of refractive index between air and metal hole array, Si_3N_4 was used as the impedance matching layer. Experimental parameter were calculated and determined in advance by the rigorous coupled wave analysis (RCWA) simulation, and then the experiment was carried out. A 2-dimensional metal hole array structures were patterned on the size of $1 \times 1 \text{ cm}^2$ GaAs substrate using photolithography process, and 5 nm thick Ti, 50 nm thick Au were deposited by E-beam evaporator, respectively. Subsequently, Si_3N_4 films with various thicknesses (150, 350, 550, and 750 nm) were deposited by plasma enhanced chemical vapor deposition (PECVD). For the comparison, transmittance of specimens with and without Si_3N_4 was measured using Fourier transform infrared spectroscopy (FTIR) in the range of 2.5 - 15 μm. Furthermore, the surface and the cross-sectional images were collected from the specimens by scanning electron microscopy (SEM) as shown in Figure 2. From the results, it is demonstrated that the transmittance is enhanced up to 80% by the deposition of 750 nm Si_3N_4 at 6.23 μm as shown in Figure 3. Based on our experimental and theoretical results, the antireflection coating layer (Si_3N_4) is used to enhance the infrared device performance.

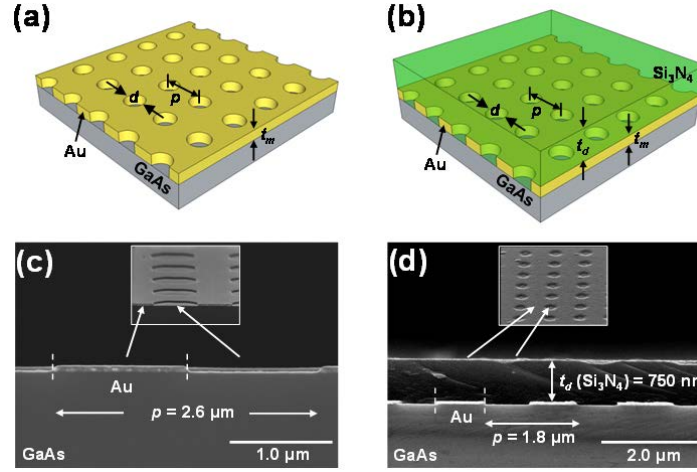


Figure 2 | Schematic layouts of Au/Ti/GaAs MHA structure (a) with and (b) without Si_3N_4 layer. The p is pitch, d is diameter, and t_d is Si_3N_4 thickness. The cross-sectional SEM images of metal hole array in Au film on GaAs substrate (c) before and (d) after PECVD of a 750-nm-thick Si_3N_4 overlayer.

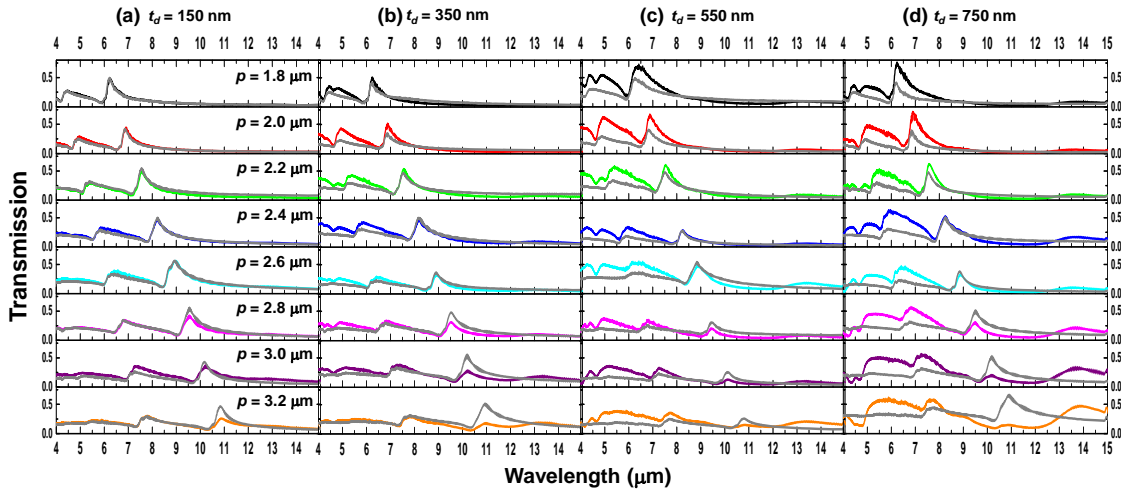


Figure 3 | Sequence of transmission spectra through the metal hole array as the pitch increases from 1.8 to 3.2 μm at 0.2 μm intervals ($d = 0.5 \cdot p$). The thickness of the PECVD Si_3N_4 overlayer increased from 150 to 750 nm at 200 nm intervals.

3. Splitting of surface plasmon resonance peaks under TE- and TM-polarized illumination (Section II-c)

We investigate experimentally and theoretically the splitting of surface plasmon (SP) resonance peaks under TE- and TM-polarized illumination. The SP structure at infrared wavelength is fabricated with a 2-dimensional square periodic array of circular holes

penetrating through Au film. In brief, the processing steps to fabricate the SP structure are as follows. (i) A standard optical lithography was performed to produce a periodic array of photoresist (PR) circular cylinders. (ii) After the PR pattern, e-beam evaporation was used to deposit a 50-nm thick layer of Au. (iii) A lift-off processing with acetone to remove the PR layer, leading to final structure (pitch, $p = 2.2 \mu\text{m}$; aperture size, $d = 1.1 \mu\text{m}$) as shown in Figure 4(a). The transmission is measured using a Nicolet FTIR at the incident angle from 0° to 36° with a step of 4° both in TE and TM polarization. Measured first and second order SP resonances at interface between Au and GaAs exhibit the splitting into two branches under TM-polarized light as shown in Figure 4(b). However, as the incidence angle under TE polarization is increased, the 1st order SP resonance peak blue-shifts slightly while the splitting of 2nd order SP resonance peak tends to be larger (not shown here). For the purpose of understanding our experimental results qualitatively, SP resonance peak wavelengths can be calculated from momentum matching condition (black circle depicted in Figure 4(b)), $\vec{k}_{sp} = \vec{k}_{\parallel} \pm i\vec{G}_x \pm j\vec{G}_y$, where \vec{k}_{sp} is the SP wavevector, \vec{k}_{\parallel} is the in-plane component of incident light wavevector, i and j are SP coupling order, and \vec{G} is the grating momentum wavevector. Moreover, for better understanding we performed 3D full field electromagnetic simulations of SP structure using a finite integration technique (CST Microwave Studio). Figure 4(b) shows an excellent agreement between the experimental, calculated and CST-simulated splitting of SP resonance peaks with various incidence angles under TM-polarized illumination (TE results are not shown here). The simulated z-component electric field (E_z) distribution at incident angle, 0° and 16° under TM polarization and at the corresponding SP resonance wavelength is shown in Figure 4(c). The analysis and comparison of modeling results with experiment indicates a good qualitative agreement of the splitting behavior of perforated Au film measured using the transmission.

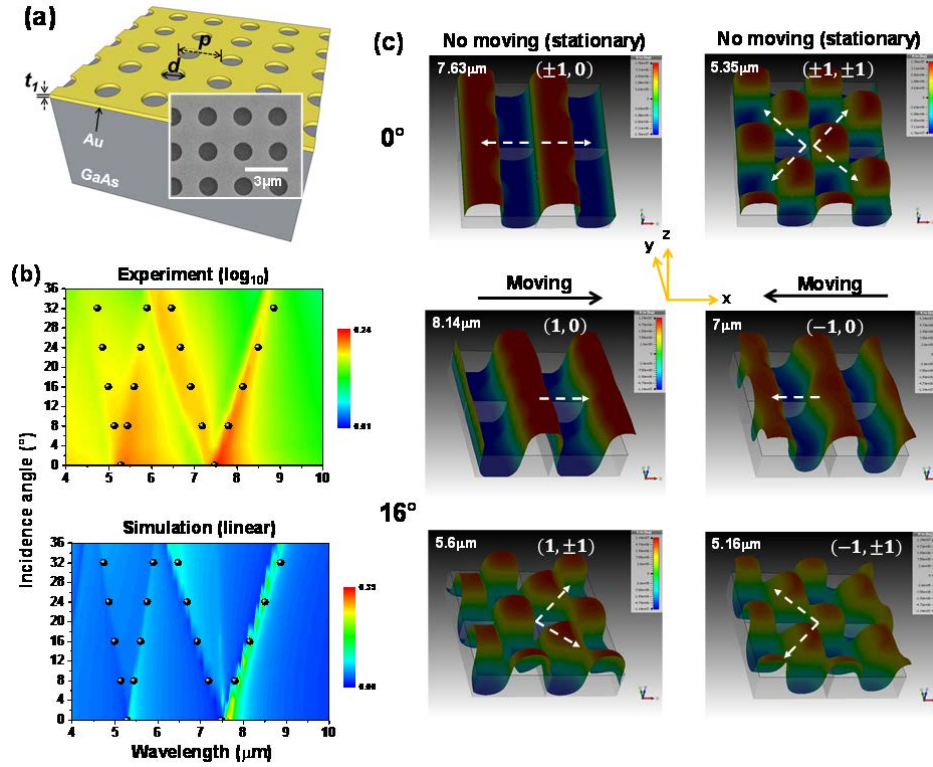


Figure 4 | (a) Schematic view of SP-structure and SEM image. (b) Experimental, calculated simulated SP resonance wavelengths as a function of TM-polarized incidence angle and wavelength. (c) Simulated E_z field distribution at corresponding SP resonance wavelengths at 0° and 16° TM incident light.

4. Improved device performance of infrared detectors based on sub-monolayer quantum dots (Section II-d)

One of the alternative growth modes to the formation of Stranski-Krastanov (SK) QDs is a sub-monolayer (SML, less than 1 monolayer) deposition technique, which can achieve a much higher density, smaller size, better uniformity, and has no wetting layer as compared to the SK growth mode. Due to the advantages of SML-QDs, the SML-DWELL design has attractive features such as increased normal incidence absorption, strong in-plane quantum confinement, and narrow spectral wavelength detection as compared with SK-DWELL.

We have investigated the effect of confinement barriers on the performance of SML-DWELL detectors whose active region is composed of 4 stacks 0.3 ML InAs with $\text{In}_{0.15}\text{Ga}_{0.85}\text{As}$ spacers. It was found that sample A with a confinement-enhanced $\text{Al}_{0.22}\text{Ga}_{0.78}\text{As}$ barrier had a single peak at 7.8 μm with a detectivity of $1.2 \times 10^{11} \text{ cm.Hz}^{1/2}/\text{W}$ ($V_b = -0.4 \text{ V}$ bias) at 77 K. However, sample B with an $\text{Al}_{0.20}\text{Ga}_{0.80}\text{As}$ barrier had three peaks at ($\sim 3.5 \mu\text{m}$, $\sim 5 \mu\text{m}$, $\sim 7 \mu\text{m}$) due to various quantum confined transitions. Sample B had a reduced dark current which improved the 77 K peak detectivity to $5.4 \times 10^{11} \text{ cm.Hz}^{1/2}/\text{W}$ although at a higher operating

bias $V_b = -1.5$ V bias. In addition, D^* of sample B under low bias (-0.6 V) is $\sim 1 \times 10^{11}$ $\text{cm.Hz}^{1/2}/\text{W}$ at both ~ 5 μm and ~ 7 μm , which is suitable for a Focal Plane Array.

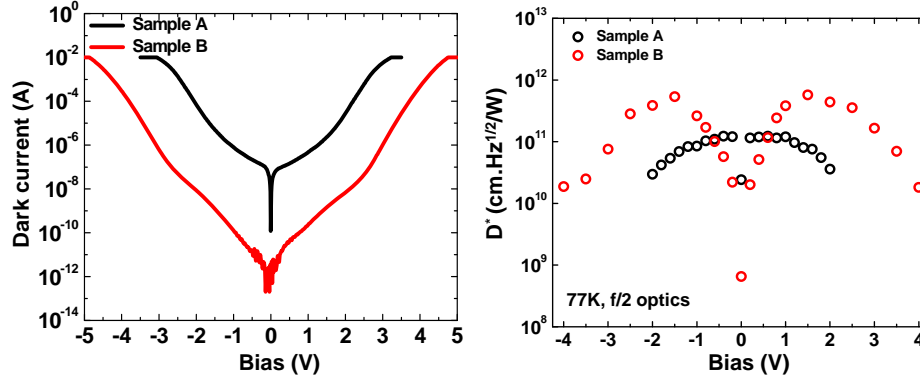


Figure 5 | (a) Dark current of sample A and B at 77 K. Dark current of sample B is lower than sample A by over 3 orders of magnitude because of the high Al composition in AlGaAs barrier as current blocking layer. (b) Detectivity of both samples at 77 K.

5. Investigation of the shape of sub-monolayer quantum dots using spectral response measured for in-plane and out-plane polarization (Section II-e)

The transmission electron microscopy (TEM), scanning TEM (STEM), and atomic force microscopy (AFM) are typically used for structural characterization. The shape of SK-QDs along $[1\bar{1}0]$ direction is slightly longer than $[110]$ direction by plane-view TEM image (This asymmetric shape of SK-QDs can be controlled by changing the growth conditions). However, the sample preparation to take TEM or STEM image can be a complex procedure and destructive. Moreover, the other technique such as AFM can determine a lateral and vertical shape of uncapped QDs, but is not possible to measure shape of QDs embedded in quantum well or barrier layer in active region of QDIP structure. For this reason, many research groups have reported in-plane (i.e., plane normal to growth direction or spanned by $[110]$ and $[1\bar{1}0]$ directions) or out-plane (i.e., plane parallel to the 45° -polished surface) polarization dependent spectral response of QDIP based on intersubband transition in SK-QDs in order to demonstrate the optical anisotropy resulting from the asymmetry of in-plane shape and aspect ratio (defined as the height divided by base) of SK-QDs. However, to the best of our knowledge the shape of QDs has not been inferred from polarization dependent spectral response to date. In this study, in-plane and out-of-plane polarized spectral responses are used to investigate the shape of sub-monolayer quantum dots in infrared photodetectors composed of 3-6 stacks 0.3 ML InAs. We found that in-plane polarization anisotropy of 5 stacks of SML-QDs (and SK-QDs) results from the asymmetric shape of QDs as shown in Figure 6. The polarization response of 5 stacks of SML-QDs (and SK-QDs), typically characterized in terms of polarization degree, is evaluated and the aspect ratio is measured using the STEM and high resolution TEM images wherein an interdiffusion of indium atoms

in 5 stacks SML-QDs is observed.

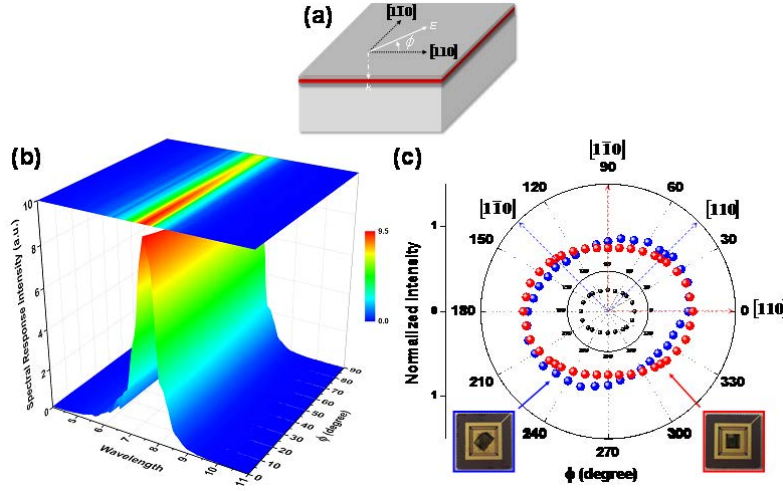


Figure 6 | (a) Illustration of normal incidence measurement of SML-QDIPs depending on incident electric field direction with defined angle (ϕ) from $[110]$. (b) ϕ dependent spectral response (SR) of #5-SML-QDIP was measured for in-plane (spanned by $[1\bar{1}0]$ and $[110]$) polarized light and at 77K operating temperature. (c) Polar plot of normalized SR-intensity at peak wavelength for #5-SML-QDIP.

6. Process optimization for plasmonic architecture and FPA (320×256) chip (Section II-f)

We have optimized the removal process of GaAs substrate in infrared QD focal plane array device as follows. (I) The substrate was thinned by mechanical lapping, followed by mechanical-chemical polishing using Chemlox (Logitech, PM5). (II) Substrate was completely removed up to the aluminum arsenide (AlAs) etch stop layer (ESL) by selective high density plasma etch (ICP: TTL-FABStar).

To obtain high etching selectivity of GaAs substrate over AlAs ESL, the variable process parameters are as follows,

- ICP source power : 0 ~ 600 W
- RF chuck power: 0 ~ 60 W
- Pressure : 1.0 ~ 50 mTorr
- Gases flow : BCl_3 (18 ~ 24 sccm)/ SF_6 (0 ~ 10 sccm)/Ar (10 sccm)

The optimized etching parameters were: BCl_3 = 22 sccm, SF_6 = 8 sccm, pressure 1.0 mTorr, RF power = 20 W, ICP power = 600 W, and substrate temperature = 25°C. The etch rate of

GaAs is 0.25 $\mu\text{m}/\text{min}$, and the selectivity close to 300.

Figure 7 shows the processing steps for substrate removal and typical images of surface after lapping, polishing and selective dry etch process.

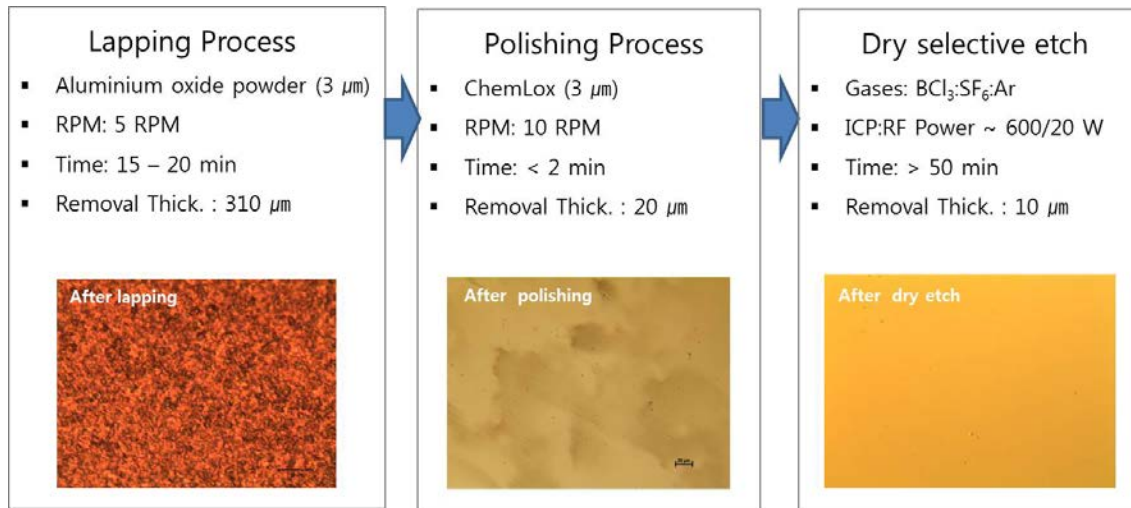


Figure 7 | Processing steps for substrate removal.